Transition between locked and running states for dimer motion induced by periodic external driving

D. Hennig, S. Martens, and S. Fugmann
Institut für Physik, Humboldt-Universität Berlin, Newtonstrasse 15, 12489 Berlin, Germany
(Received 1 April 2008; published 3 July 2008)

We study the motion of a dimer in a one-dimensional spatially periodic washboard potential. The tilt of the latter is time-periodically modulated by an ac field. We focus interest on the detrapping of the (static) ground state solution of the dimer caused by the ac field. Moreover, we demonstrate that slow tilt modulations not only induce a trapping-detrapping transition but drive the dimer dynamics into a regime of transient long-range running states. Most strikingly, the motion proceeds then unidirectionally, so that the dimer covers huge distances regardless of the fact that the bias force in the driven system vanishes on the average. We elucidate the underlying dynamics in phase space and associate long-lasting running states with the motion in ballistic channels occurring due to stickiness to invariant tori.

DOI: 10.1103/PhysRevE.78.011104 PACS number(s): 05.60.Cd, 05.45.Ac, 05.45.Pq

I. INTRODUCTION

Transport phenomena play a fundamental role in many physical systems. In this context the so-called washboard potential, due to its ubiquity and simplicity, establishes the prototype of a periodic potential and is employed in a number of applications, including Josephson junctions [1], charge density waves [2], superionic conductors [3], rotation of dipoles in external fields [4], phase-locked loops [5], and diffusion of dimers on surfaces [6–12] to quote a few. By application of an external time-periodic driving to the washboard potential, interesting effects such as phase-locking, hysteresis [13], and stochastic resonance [14] are found. Recent investigations have dealt with the particle movement in a washboard potential whose tilt is time-periodically varied by a weak external modulation field [15–18]. It has been demonstrated that adiabatic modulations of the tilt lead to the generation of transient transport dynamics related to enormous directed particle flow. An explanation for this behavior has been given in terms of the underlying phase space structure of the driven one-degree-of-freedom system promoting the motion in ballistic channels [19].

In this paper, we study an extension of previous work on individual particle (monomer) dynamics and consider the case when two particles interact due to harmonic coupling, constituting a dimer. For nonvanishing coupling strength, pronounced relative vibrations of the monomer-monomer distance are possible. On the other hand, in the limit of strong monomer-monomer coupling, distance vibrations are inhibited and thus the resulting rigid dimer reduces to a one-particle system, viz., effectively a monomer. The driven dynamics of the latter can be treated in the same manner as mentioned in [15–18]. Considering intermediate coupling strengths, we focus interest on nonrigid dimers exhibiting distance vibrations. Motion takes place in a phase space for which details of the intricate structures remain elusive, not least due to the higher dimensionality. Whether in systems with a larger number of (microscopic) degrees of freedom such (macroscopic) behavior as collective motion leading to a directed flow emanates from higher-dimensional dynamics is not obvious. It is the objective of the current work to explore under which conditions in a system of coupled particles the generation of a directed flow going along with collective motion is possible.

II. MODEL OF THE DRIVEN DIMER SYSTEM

We study the dimer dynamics with a Hamiltonian of the form

$$H = \sum_{n=1}^{2} \left(\frac{p_n^2}{2} + U_0(q_n) + U_1(q_n,t) \right) + \frac{\kappa}{2}(q_2 - q_1 - l_0)^2, \quad (1)$$

wherein p_n and q_n, $n=1,2$, denote the canonically conjugate momenta and positions of the two coupled particles evolving in a periodic, spatially symmetric, washboard potential of unit period given by

$$U_0(q) = U_0(q+1) = -\cos(2\pi q)/(2\pi). \quad (2)$$

The external, time-dependent forcing field

$$U_1(q_n,t) = -F \sin(\Omega t + \Theta_0) q_n \quad (3)$$

causes time-periodic modulations of the tilt of the washboard potential. It has to be stressed that there is no bias force involved in the sense that the following average over time and space vanishes, i.e.,

$$\int_0^1 dq \int_0^{T=2\pi/\Omega} dt \frac{\partial U(q,t)}{\partial q} = 0, \quad (4)$$

with $U(q,t)=U_0(q)+U_1(q,t)$. The two monomers interact harmonically with coupling strength κ. The parameter l_0 denotes their equilibrium distance.

For a discussion of the dynamics it is convenient to introduce the following canonical change of variables induced by the generating function: $S=\frac{1}{2}(q_1+q_2)P_x+\frac{1}{2}(q_1-q_2)P_y$, relating the old and new variables as

$$p_1 = \frac{1}{2}(P_x + P_y), \quad p_2 = \frac{1}{2}(P_x - P_y), \quad (5)$$

$$Q_x = \frac{1}{2}(q_1 + q_2), \quad Q_y = \frac{1}{2}(q_1 - q_2). \tag{6}$$

The Hamiltonian expressed in the new variables becomes

$$H = \frac{1}{4}(P_x^2 + P_y^2) - \frac{1}{\pi}\cos(2\pi Q_x)\cos(2\pi Q_y) + \frac{\kappa}{2}(2Q_y + l_0)^2 - 2F\sin(\Omega t + \Theta_0)Q_x. \tag{7}$$

The corresponding equations of motion, describing the effective motion of a particle in a two-dimensional potential landscape, are given by

$$\ddot{Q}_x = -\cos(2\pi Q_y)\sin(2\pi Q_x) + F\sin(\Omega t + \Theta_0), \tag{8}$$

$$\ddot{Q}_y = -\cos(2\pi Q_x)\sin(2\pi Q_y) - \kappa(2Q_y + l_0). \tag{9}$$

Evidently, the impact of the external modulation and the harmonic coupling occurs in separate equations. The coupling between the Q_x and Q_y degrees of freedom results from parametric modulations of the respective potential force term. Apart from that, Eq. (8) for the mean value Q_x is equivalent to the equation $\ddot{q}+\sin(2\pi q)-F\sin(\Omega t+\Theta_0)=0$ of the driven single-particle case [15,17,18]. Remarkably, as pointed out in prior literature [15,16], in a system of uncoupled particles, i.e., $\kappa=0$, there results an (unexpected) asymmetry of the flux of particles, emanating from one potential well and flowing to the left and right potential wells, which indicates the existence of directed transport without breaking the reflection symmetry in space and time in this system. One reason for the occurrence of phase-dependent directed transport is the lowering of the symmetry of the flow in phase space by the ac field, where this asymmetry vanishes only for specific values of the initial phase Θ_0 [15].

Due to the similarity between Eq. (8) and the equation of the driven single-particle case, we surmise that the external modulation leads to an escape of particles from a potential well, inducing ongoing rotational motion of the mean value Q_x equivalent to the behavior observed in the study of driven monomer dynamics [18]. In contrast to that, the amplitude of the difference variable Q_y is bounded due to the harmonic restoring force associated with the κ term in Eq. (9).

In the following we explore whether it is indeed possible to detrap the dimer through the impact of a time-dependent external modulation. The amplitude F of the tilt modulation term is supposed to be undercritical in the sense that the two coupled monomers remain trapped in a potential well of the potential with *static* positive as well as negative tilt, i.e., when $U(q_n)=U_0(q_n)\pm Fq_n$. In other words only for time-dependent modulations is escape from the potential well possible due to the arising chaotic dynamics [18]. More precisely, the trajectory has to be in the stochastic region emerging around the separatrix in phase space, so that crossing from the interior separatrix region (trapped solutions) to the outer separatrix region (detrapped solutions) can take place [18].

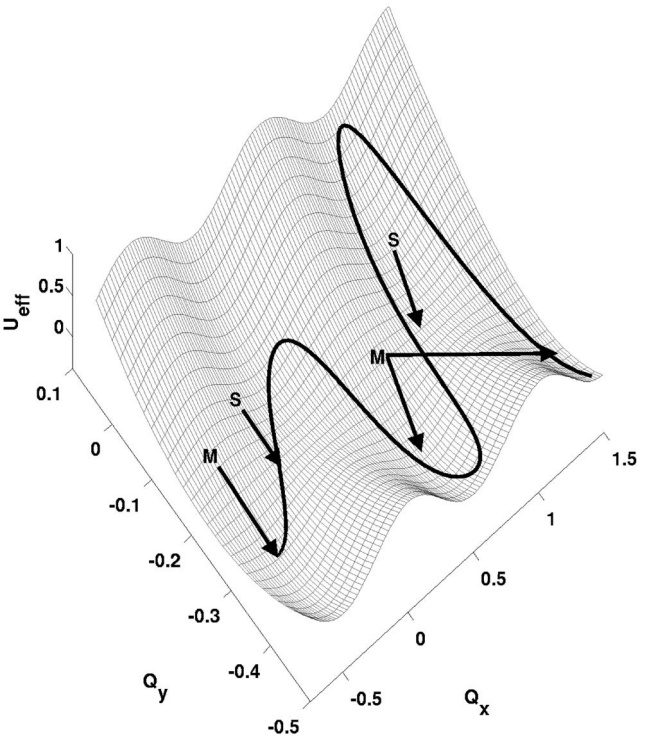

FIG. 1. Barrier crossing of the trajectory of the dimer emanating from the minimum, labeled as M, in one potential well and passing through a saddle, labeled as S, represented by the wiggling solid line. The untilted potential energy landscape $U_{\mathrm{eff}}(Q_x,Q_y)$ is additionally depicted. The parameter values are $l_0=0.5$, $\kappa=5$, $F=0.4$, $\Omega=10^{-3}$, and $\Theta_0=0$.

III. INITIAL CONFIGURATION AND POTENTIAL LANDSCAPE

For our dynamical studies it is assumed that the dynamics starts off with zero tilt of the potential, i.e., $\Theta_0=0$. In Fig. 1 we illustrate the motion of the dimer in the potential landscape U_{eff} related to the potential term in Eq. (7),

$$U_{\mathrm{eff}} = -\frac{1}{\pi}\cos(2\pi Q_x)\cos(2\pi Q_y) + \frac{\kappa}{2}(2Q_y + l_0)^2. \tag{10}$$

The dimer is initially locked in its ground state, attained without exerted tilt ($F=0$). The trajectory in Fig. 1, starting from the potential minimum (ground state), passes from one well to a neighboring one by crossing a saddle point in between.

The corresponding stationary states $\{\tilde{Q}_x,\tilde{Q}_y\}$ are derived from Eqs. (8) and (9) with $\ddot{Q}_x=\ddot{Q}_y=0$, yielding two sets

$$\tilde{Q}_x^m = \frac{1}{2}m, \quad m \in \mathbb{Z}, \tag{11a}$$

$$\tilde{Q}_y^m = -\frac{1}{2}\left(\frac{(-1)^m\sin(2\pi\tilde{Q}_y^m)}{\kappa} + l_0\right), \quad m \in \mathbb{Z}, \tag{11b}$$

$$\tilde{Q}_x^n = \frac{1}{2\pi}\arccos\left[(-1)^{n+1}\kappa\left(\frac{1}{2} + n + l_0\right)\right], \tag{12a}$$

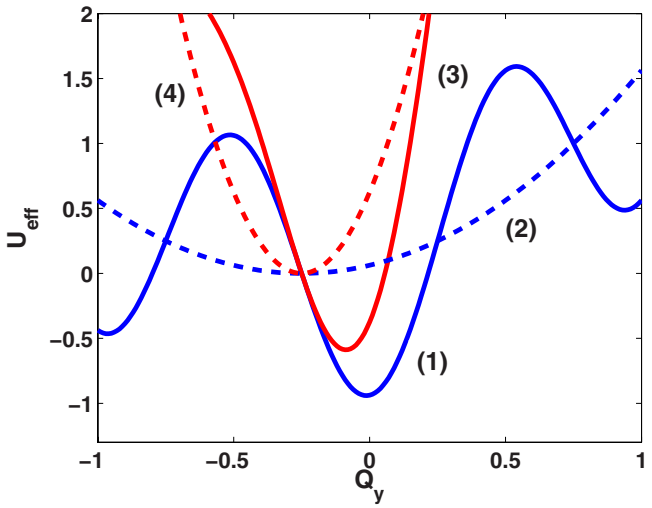

FIG. 2. (Color online) Potential energy U_{eff} as a function of the difference coordinate Q_y for fixed $Q_{x,g}=0$ (labeled 1 and 3 for coupling strength $\kappa=0.5$ and 5, respectively) and fixed $Q_{x,s}=0.25$ (labeled 2 and 4) for coupling strength $\kappa=0.5$ and 5, respectively). The minimum of the graphs 1 and 3 determines the position of the ground state $Q_{y,g}$ while for the graphs 2 and 4 the minimum lies at the value of the saddle point $Q_{y,s}=-l_0/2=-0.25$. The remaining parameter values are $l_0=0.5$ and $F=0$.

$$\tilde{Q}_y^n = \frac{1}{4} + \frac{1}{2}n, \quad n \in \mathbb{Z}. \tag{12b}$$

Provided that the inequality

$$\kappa^2\left(\frac{1}{2} + n + l_0\right)^2 \leq 1, \quad n \in \mathbb{Z}, \tag{13}$$

is satisfied, it can be shown that the stationary points $\{\tilde{Q}_x^n, \tilde{Q}_y^n\}$ are of hyperbolic and $\{\tilde{Q}_x^m, \tilde{Q}_y^m\}$ are of elliptic type. The latter represents the ground state, since $U_{\text{eff}}(\tilde{Q}_x^m, \tilde{Q}_y^m) < U_{\text{eff}}(\tilde{Q}_x^n, \tilde{Q}_y^n)$. Otherwise, if the inequality (13) is not satisfied, the only possible stationary states are represented by $\{\tilde{Q}_x^m, \tilde{Q}_y^m\}$. Regarding the ground state in the latter situation the following cases have to be considered: If $l_0 \leq 0.5$, the ground state is attained for even m, whereas for $l_0 > 0.5$ m is odd.

In the following, due to symmetry in the x direction it is sufficient to consider only the motion of the dimer in the range $Q_x \in [0,1)$, which is equivalent to $m=0,1$ and $n=-1$ in the expressions (11a), (11b), (12a), and (12b). We denote the ground state by $\{Q_{x,g}, Q_{y,g}\}$ and its energy with E_g. Likewise, for the saddle point $\{Q_{x,s}, Q_{y,s}\}$ and its energy is E_s.

In order to overcome the local potential barrier, the dimer has to gain sufficient energy from the external modulation field. The height of the potential barrier is determined by $\Delta E = E_s - E_g$. ΔE varies with the coupling strength as illustrated in Fig. 2, where the potential $U_{\text{eff}}(Q_x, Q_y)$ as a function of the difference coordinate Q_y is drawn for the fixed ground state value $Q_{x,g}=0$ for coupling strength $\kappa=0.5$ (graph labeled as 1) and $\kappa=5$ (graph labeled as 3). The minimum value of the potentials corresponds to the respective ground state energy. In addition, $U_{\text{eff}}(Q_{x,s}=1/4, Q_y)$ is depicted and labeled 2 for $\kappa=0.5$ and 4 for $\kappa=5$. The energy of the saddle point is determined by the minimum value of the graphs 2 and 4. For the lower coupling strength $\kappa=0.5$, not only is the distance between the positions of the minima of the graphs of $U_{\text{eff}}(0, Q_y)$ and $U_{\text{eff}}(1/4, Q_y)$ comparatively large, but also a fairly high difference between the minimal energy levels results. In comparison, for increased coupling strength $\kappa=5$ the minima of the corresponding potential curves 3 and 4 are close together and the energetic gap is considerably lower than in the preceding case. This becomes clear from Eq. (12a). The position of the saddle point and the potential energy are independent of the coupling strength κ for the chosen values $l_0=0.5$ and $n=-1$. In contrast, the location of the ground state and the corresponding energy value depend on κ. The position $Q_{y,g}$ is given by the transcendent equation (11b). The amplitude of the sinusoidal term decreases with increasing coupling strength. Hence, the value of the difference coordinate at the ground state shifts from $Q_{y,g} \simeq 0$ for $\kappa \simeq 0$ to $Q_{y,g} \simeq -l_0/2$ with further increasing coupling strength, so that the position of the saddle point $Q_{y,s}=-l_0/2$ is approached. On the other hand, according to Eq. (10), the corresponding potential energy in the ground state increases with the value of κ. From this it follows that the energetic gap is considerably lower in the case of stronger coupling.

This energy gap determines the energy barrier that the dimer has to overcome in the Q_x direction in order to accomplish motion of the mean coordinate Q_x from one potential well into the neighboring one, a behavior that is called detrapping. For a low coupling strength $\kappa=0.5$, the relative energy gap is $\Delta E/E_{\text{barrier}} \simeq 2.9$ whereas for a stronger coupling strength $\kappa=5$ the ratio reduces to $\Delta E/E_{\text{barrier}} \simeq 1.8$. $E_{\text{barrier}}=1/\pi$ is the barrier height of the washboard potential given in Eq. (2).

IV. FIELD-INDUCED TRAPPING-DETRAPPING TRANSITIONS

We performed extensive studies of the parameter dependence of the modulation-induced escape of the dimer from its ground state. As Fig. 3 reveals, in a certain range for the equilibrium length, escape from the ground state is achieved provided that a critical coupling strength is exceeded, which is related to a sufficiently low ΔE. Interestingly—regarding the detrapping of the dimer—the choice of the modulation frequency plays no important role. We observed barrier crossing of the dimer in a wide range of the modulation frequency.

However, it should be stressed that not all escapes from the potential well lead necessarily to unidirectional motion of the dimer, i.e., a running solution persisting throughout our long simulation time of $t=10^6$. This becomes evident from Fig. 4 where the time evolution of the mean coordinate Q_x is displayed for several values of the modulation frequency. The coupling strength $\kappa=5$ is chosen such that in accordance with Fig. 3 detrapping of the dimer is assured for time-periodic modulations of the tilt. For modulations with $\Omega=1$, the dimer does not get far away from its initial position, while for lower frequencies $\Omega=0.1$ and 0.01 considerably

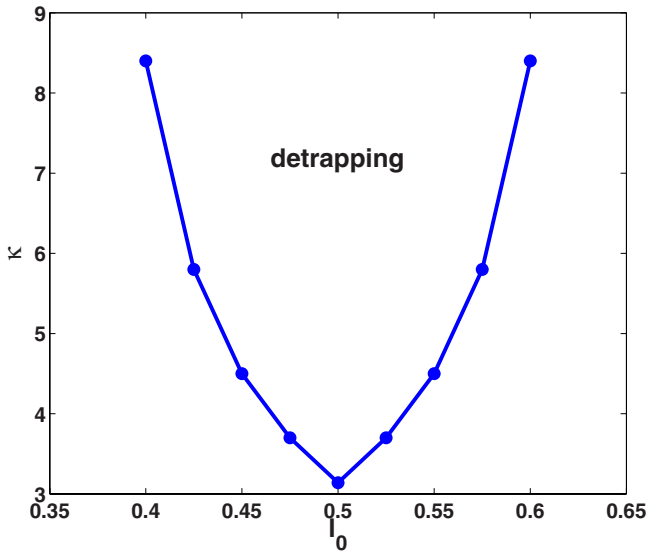

FIG. 3. (Color online) Critical coupling strength for dynamical detrapping as a function of the equilibrium length. The parameter values are $F=0.4$ and $\Theta_0=0$. For the choice of Ω we refer to the text.

long distances away from the initial position are covered but the motion does not proceed unidirectionally. By comparison, for slower modulations with $\Omega=10^{-3}$ and strong enough coupling, illustrated here for $\kappa=5$ and 10, the dimer motion proceeds with virtually constant velocity directed over a huge distance, as seen in the bottom panel of Fig. 4. (For comparison, the trajectory is also displayed for an undercritical coupling strength of $\kappa=3.14$ for which no enhanced propagation occurs.) In such cases the difference variable Q_y typically performs quasiregular oscillations with a maximal amplitude in a certain interlude, at the end of which the maximal amplitude changes rather abruptly to a new value. As a consequence, the distance between monomers varies such that occasionally one of the monomers overtakes the other one as depicted in Fig. 5.

Moreover, in Fig. 1 it is clearly seen that the first escape path goes from the minimum through a saddle point into the next potential valley. For subsequent escapes the dimer, having gathered meanwhile more energy from the modulation field, is enabled to pass the potential barriers near the corresponding saddles.

To gain more insight into the dynamics in the five-dimensional phase space spanned by the variables $(P_x,P_y,Q_x,Q_y,\Theta=\Omega t)$, we utilize Poincaré plots where the cross section is determined as follows:

$$\Sigma:=\{(P_x,Q_x,\Theta)|Q_y=0,P_y>0\}. \tag{14}$$

We represent in Fig. 6 Poincaré plots projected on the Θ-P_x plane corresponding to the dynamics shown in Fig. 4. The top panel shows the result for a driving with $\Omega=1$ while in the bottom panel the modulation frequency is $\Omega=10^{-3}$. Clearly, in the former case the traversed momentum range is not only rather strongly confined but also virtually symmetric with respect to $P_x=0$ and thus no direction of motion is distinguished (cf. also Fig. 4). In contrast to this for adiabatic

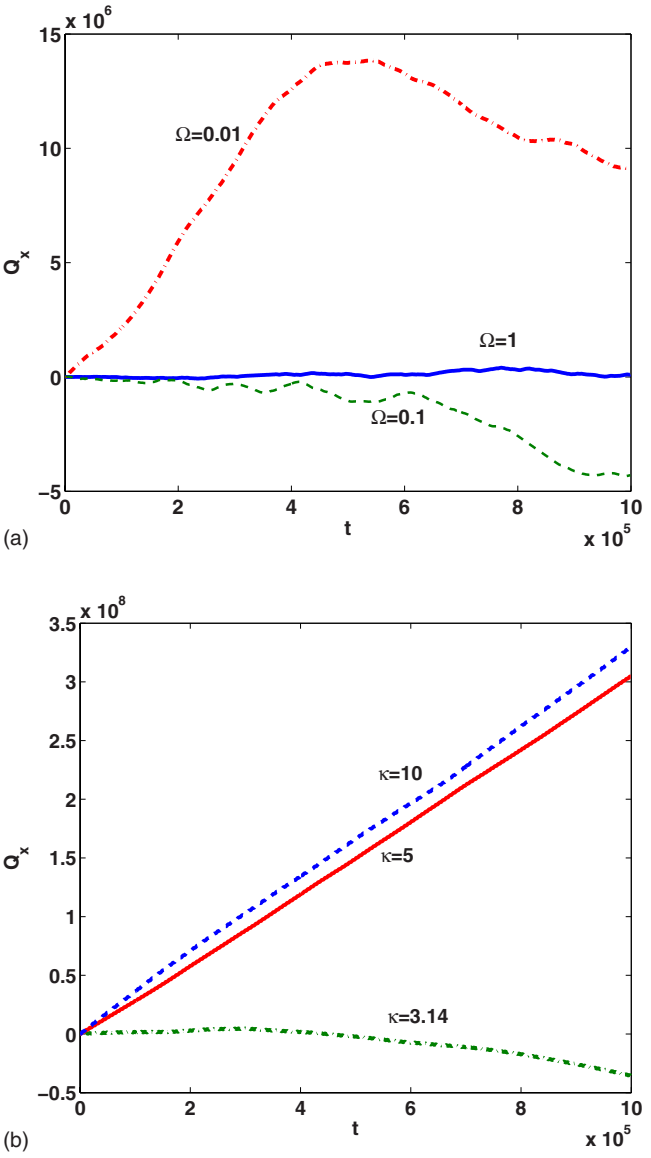

FIG. 4. (Color online) Time evolution of the center of mass coordinate Q_x. Left panel: Fixed coupling strength $\kappa=5$ and various modulation frequencies as indicated in the plot. Right panel: Fixed $\Omega=10^{-3}$ and different values of κ as indicated in the plot. The remaining parameter values are $l_0=0.5$ and $F=0.4$.

modulations with $\Omega=10^{-3}$ the momentum P_x experiences vast alterations in dependence on the value of the phase Θ. To be precise, starting from an unbiased potential, i.e., $\Theta_0=0$, the force term $F(t)=F\sin(\Omega t)$ produces a negative tilt of the potential in the interval $0<t\leq\pi/\Omega$. It happens that at some instant of time $t_{\text{escape}}\leq\pi/(2\Omega)$ the coordinate Q_x overcomes the potential barrier and even escapes from the well. Hence there remains a time interval $[t_{\text{escape}},\pi/\Omega]$ during which the dimer still experiences a force with positive sign which further enhances the motion in the right direction toward increasing values of Q_x. For times $\pi/\Omega<t\leq2\pi/\Omega$, the force $F(t)=F\sin(\Omega t)$ acts in the opposite direction. In particular, for $2\pi/\Omega-t_{\text{escape}}\leq t\leq2\pi/\Omega$ the momentum evolves with its sign reversed compared to the previous enhancement period. With this we can estimate the gain in momentum as follows:

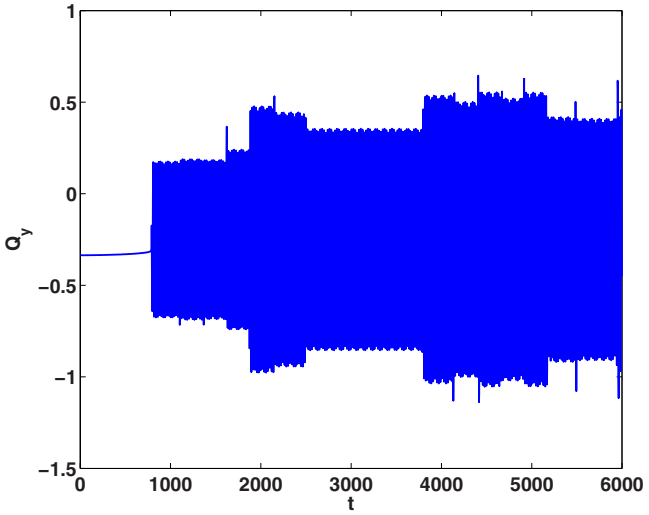

FIG. 5. (Color online) Time evolution of the difference coordinate Q_y. The parameter values are $l_0=0.5$, $\kappa=5$, $F=0.4$, $\Omega=10^{-3}$, and $\Theta_0=0$.

$$\Delta P_x = \left(\int_{t_{\text{escape}}}^{\pi/\Omega} + \int_{2\pi/\Omega - t_{\text{escape}}}^{2\pi/\Omega} \right) d\tau \dot{p}$$
$$= \left(\int_{t_{\text{escape}}}^{\pi/\Omega} + \int_{2\pi/\Omega - t_{\text{escape}}}^{2\pi/\Omega} \right) d\tau [-\sin(2\pi Q_x)\cos(2\pi Q_y) + F\sin(\Omega\tau)]. \quad (15)$$

For small Ω the rapidly oscillating part connected with the first term in the integral averages to zero, and we find

$$\Delta P_x = 2\frac{F}{\Omega}\cos(\Omega t_{\text{escape}}). \quad (16)$$

In general, the smaller Ω the higher is the gain in momentum; see also [15,17].

We briefly discuss the formation of the directed motion. With this aim we relate the dynamics to the underlying structures in phase space. In the driven monomer dynamics, arising for vanishing coupling $\kappa=0$, the phase space is three dimensional. Chaotic trajectories, meandering in the arising stochastic layer, can stick to the border of islands of regular motion for considerably long times [20,21]. This is due to the intricate structure of the stochastic layer, where close to resonances at the boundary between regular and chaotic regions there exists a hierarchy of smaller and smaller islands and surrounding cantori. The latter can severely restrict the transport in phase space and thus effectively partition the chaotic layer [21]. Particularly for motion trapped in the vicinity of islands of stability with nonzero winding number (ballistic channels), directed motion in the q direction is enhanced [17–19].

For nonlinear Hamiltonian systems with $N \geq 2$ degrees of freedom only a few numerical results addressing the existence of an enhanced trapping regime are known [22,23]. It is supposed that the role played by cantori in driven systems with $N=1$ is played by families of N-dimensional tori, constituting partial barriers in the $2N$-dimensional phase space, to which the chaotic trajectory can stick [22].

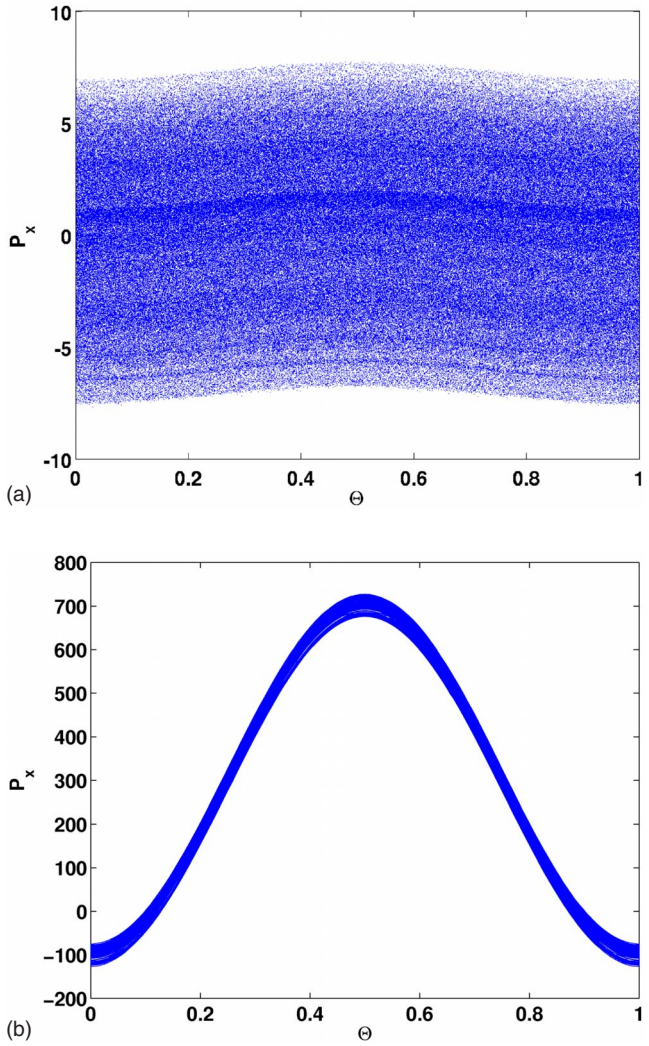

FIG. 6. (Color online) Poincaré plots presented in the Θ-P_x plane. The phase variable Θ is given mod(2π). Illustrated are a driving with $\Omega=1$ (top panel) and an adiabatic driving with $\Omega=10^{-3}$ (bottom panel). The remaining parameter values are $l_0=0.5$, $\kappa=0.5$, $F=0.4$, and $\Theta_0=0$.

For the driven dimer system with its five-dimensional phase space, Arnold diffusion is possible. Hence in principle a chaotic trajectory can wander along the entire stochastic layer, so exploring eventually the whole phase space [24–27]. However, due to stickiness to higher-dimensional invariant tori, Arnold diffusion can be severely suppressed so that certain regions are distinguished in which the trajectories become trapped for longer times [22]. In fact, our findings (cf. Fig. 6) indicate that in the adiabatically driven dimer system the trajectories are captured in ballistic channels associated with stickiness to two-dimensional invariant tori, leading to long-lasting directed motion. This is further underpinned by the fact that in the dimer system the mean value Q_x evolves in the same manner as the single coordinate q in the monomer counterpart, viz., it exhibits gigantic growth over a long period of time, implying that motion takes place in ballistic channels [18].

V. SUMMARY

In conclusion, we have shown that it is possible to detrap the ground state of a dimer in a washboard potential through time-periodic modulations of its tilt. Moreover, when the tilt modulations vary, adiabatically directed transport of the dimer, viz., a running state, is initiated. Most importantly, unidirectional motion of the dimer prevails over a very long period of time. In terms of phase-space dynamics we have found evidence that this phenomenon is linked with enhanced trapping of the trajectories around families of invariant tori. For systems involving many more degrees of freedom than in the dimer case, the issue of stickiness of invariant tori in high-dimensional phase space needs to be explored in much more detail. In particular, it has to be determined whether a macroscopic feature such as directed collective transport, which is related to motion in ballistic channels, is exhibited by systems with many microscopic degrees of freedom.

ACKNOWLEDGMENTS

This research was supported by SFB 555 and the VW Foundation Project No. I/80425. We also acknowledge very insightful and constructive discussions with L. Schimansky-Geier.

[1] A. Barone and G. Paternó, *Physics and Applications of the Josephson Effect* (Wiley, New York, 1982).
[2] G. Gruner, A. Zawadowski, and P. M. Chaikin, Phys. Rev. Lett. **46**, 511 (1981).
[3] P. Fulde, L. Pietronero, W. R. Schneider, and S. Strässler, Phys. Rev. Lett. **35**, 1776 (1975).
[4] D. Reguera, J. M. Rubí, and A. Pérez-Madrid, Phys. Rev. E **62**, 5313 (2000).
[5] C. W. Lindsey, *Synchronization Systems in Communication and Control* (Prentice-Hall, Englewood Cliffs, NJ, 1972).
[6] D. Agassi and J. H. Eberly, Phys. Rev. Lett. **54**, 34 (1985).
[7] O. M. Braun, Surf. Sci. **230**, 262 (1990).
[8] E. Pijper and A. Fasolino, Phys. Rev. B **72**, 165328 (2005).
[9] O. M. Braun, R. Ferrando, and G. E. Tommei, Phys. Rev. E **68**, 051101 (2003).
[10] E. Heinsalu, M. Patriarca, and F. Marchesoni, Phys. Rev. E **77**, 021129 (2008).
[11] M. Partriarca and P. Szelestey, Acta Phys. Pol. B **36**, 1745 (2005).
[12] C. Fusco and A. Fasolino, Thin Solid Films **428**, 34 (2003).
[13] M. Borromeo, G. Costantini, and F. Marchesoni, Phys. Rev. Lett. **82**, 2820 (1999).
[14] L. Gammaitoni, P. Hänggi, P. Jung, and F. Marchesoni, Rev. Mod. Phys. **70**, 223 (1998).
[15] O.M. Yevtushenko, S. Flach and K. Richter, Phys. Rev. E **61**, 7215 (2000).
[16] I. Goychuk and P. Hänggi, J. Phys. Chem. B **105**, 6642 (2001).
[17] S. M. Soskin, O. M. Yevtushenko, and R. Mannella, Phys. Rev. Lett. **95**, 224101 (2005).
[18] D. Hennig, L. Schimansky-Geier, and P. Hänggi, Eur. Phys. J. B **62**, 493 (2008).
[19] S. Denisov and S. Flach, Phys. Rev. E **64**, 056236 (2001); S. Denisov, J. Klafter, M. Urbakh, and S. Flach, Physica D **170**, 131 (2002); S. Denisov, J. Klafter, and M. Urbakh, Phys. Rev. E **66**, 046217 (2002).
[20] M. Zaslavsky, *Chaos in Dynamical Systems* (Harwood, New York, 1985); *Physics of Chaos in Hamiltonian Systems* (Imperial College Press, London, 1998).
[21] R. S. MacKay, J. D. Meiss, and I. C. Percival, Physica D **13**, 55 (1984); J. D. Meiss and E. Ott, *ibid.* **20**, 387 (1986).
[22] H. Kantz and P. Grassberger, Phys. Lett. A **123**, 437 (1987); M. Ding, T. Bountis, and E. Ott, *ibid.* **151**, 395 (1990); E. G. Altmann and H. Kantz, Europhys. Lett. **78**, 10008 (2007).
[23] K. Kaneko and T. Konishi, Phys. Rev. A **40**, 6130 (1989).
[24] V. I. Arnold, Sov. Math. Dokl. **2**, 245 (1961); **5**, 581 (1964).
[25] B. V. Chirikov, Phys. Rep. **52**, 263 (1979).
[26] A. J. Lichtenberg and M. A. Lieberman, *Regular and Stochastic Motion* (Springer, New York, 1983).
[27] M. Falcioni, U. M. B. Marconi, and A. Vulpiani, Phys. Rev. A **44**, 2263 (1991).